Antiviral Mechanisms and Preclinical Evaluation of Amantadine Analogs that Continue to Inhibit Influenza A Viruses with M2^{S31N}-Based Drug Resistance

Ian Tietjen, Daniel C. Kwan, Annett Petrich, Roland Zell, Ivi Theodosia Antoniadou, Agni Gavriilidou, Christina Tzitzoglaki, Michail Rallis, David Fedida, Francesc X. Sureda, Cato Mestdagh, Lieve Naesens, Salvatore Chiantia, F. Brent Johnson, Antonios Kolocouris

PII: S0166-3542(25)00030-0

DOI: https://doi.org/10.1016/j.antiviral.2025.106104

Reference: AVR 106104

To appear in: *Antiviral Research*

Received Date: 11 September 2024

Revised Date: 8 January 2025

Accepted Date: 10 February 2025

Please cite this article as: Tietjen, I., Kwan, D.C., Petrich, A., Zell, R., Antoniadou, I.T., Gavriilidou, A., Tzitzoglaki, C., Rallis, M., Fedida, D., Sureda, F.X., Mestdagh, C., Naesens, L., Chiantia, S., Johnson, F.B., Kolocouris, A., Antiviral Mechanisms and Preclinical Evaluation of Amantadine Analogs that Continue to Inhibit Influenza A Viruses with M2^{S31N}-Based Drug Resistance, *Antiviral Research*, https://doi.org/10.1016/j.antiviral.2025.106104.

Antiviral Mechanisms and Preclinical Evaluation of Amantadine Analogs that Continue to Inhibit Influenza A Viruses with M2^{S31N}-Based Drug Resistance

Ian Tietjen,[a,b,*] Daniel C. Kwan,[b] Annett Petrich,[c,d] Roland Zell, [e] Ivi Theodosia Antoniadou,[f,g] Agni Gavriilidou,[h] Christina Tzitzoglaki,[h] Michail Rallis,[f] David Fedida,[b] Francesc X. Sureda,[i] Cato Mestdagh,[j] Lieve Naesens,[j] Salvatore Chiantia,[c] F. Brent Johnson,[k] and Antonios Kolocouris [g,*]

[a] The Wistar Institute, Philadelphia, PA, 19104, USA

[b] Department of Anesthesiology, Pharmacology and Therapeutics, University of British Columbia, Vancouver, British Columbia, V6T 1Z3, Canada

[c] Institute of Biochemistry and Biology, University of Potsdam, Karl-Liebknecht-Str. 24-25, 14476, Potsdam, Germany

[d] Department of Infectious Diseases, Section of Virology, Heidelberg University, Im Neuenheimer Feld 344, 69120, Heidelberg, Germany

[e] Jena University Hospital, Institute for Medical Microbiology, Section Experimental Virology, Hans Knoell Str. 2, D-07745 Jena, Germany

[f] Laboratory of Pharmaceutical Technology, Section of Pharmaceutical Technology, Department of Pharmacy, National and Kapodistrian University of Athens, Panepistimiopolis-Zografou, 15771, Athens, Greece

[g] Biomedical Research Foundation of the Academy of Athens, 4 Soranou Ephessiou Str., 115 27 Athens, Greece;

[h] Laboratory of Medicinal Chemistry, Section of Pharmaceutical Chemistry, Department of Pharmacy, National and Kapodistrian University of Athens, Panepistimiopolis-Zografou, 15771, Athens, Greece

[i] Department of Basic Medical Sciences, Faculty of Medicine and Life Sciences, Universitat Rovira i Virgili, 43201 Reus, Spain

[j] Rega Institute, KU Leuven, Department of Microbiology, Immunology and Transplantation, B-3000 Leuven, Belgium

[k] Department of Microbiology and Molecular Biology, Brigham Young University, Provo, UT 84602, United States

[*]Corresponding Author: Ian Tietjen, itietjen@wistar.org; Antonios Kolocouris, ankol@pharm.uoa.gr

Abstract

To better manage seasonal and pandemic influenza infections, new drugs are needed with enhanced activity against amantadine- and rimantadine-resistant influenza A virus (IAV) strains containing the S31N variant of the viral M2 ion channel ($M2^{S31N}$). Here we tested 36 amantadine analogs against a panel of viruses containing either $M2^{S31N}$ or the parental, M2 S31 wild-type variant ($M2^{WT}$). We found that several analogs, primarily those with sizeable lipophilic adducts, inhibited up to three $M2^{S31N}$-containing viruses with activities at least 5-fold lower than rimantadine, without inhibiting $M2^{S31N}$ proton currents or modulating endosomal pH. While $M2^{WT}$ viruses in passaging studies rapidly gained resistance to these analogs through the established M2 mutations V27A and/or A30T, resistance development was markedly slower for $M2^{S31N}$ viruses and did not associate with additional M2 mutations. Instead, a subset of analogs, exemplified by 2-propyl-2-adamantanamine (**38**), but not 2-(1-adamantyl)piperidine (**26**), spiro[adamantane-2,2'-pyrrolidine] (**49**), or spiro[adamantane-2,2'-piperidine] (**60**), inhibited cellular entry of infectious IAV following pre-treatment and/or H1N1 pseudovirus entry. Conversely, an overlapping subset of the most lipophilic analogs including compounds **26**, **49**, **60**, and others, disrupted viral M2-M1 protein colocalization required for intracellular viral assembly and budding. Finally, a pilot toxicity study in mice demonstrated that **38** and **49** were tolerated at 30 mg/kg. Together, these results indicate that amantadine analogs act on multiple, complementary mechanisms to inhibit replication of $M2^{S31N}$ viruses.

Keywords

Influenza A virus, M2 protein, drug resistance, amantadine analogs, antiviral mechanisms of action

Highlights

- Current IAVs have M2 mutations that confer resistance to amantadine and rimantadine
- Several amantadine analogs inhibit these viruses without acting on M2 proton currents
- Alternative antiviral targets include IAV entry and M2-M1 protein colocalization
- Amantadine analogs are also tolerated in mice
- Future amantadine antivirals could simultaneously act on multiple IAV mechanisms

1. Introduction

Despite the wide accessibility of seasonal vaccines, influenza A virus (IAV) remains a significant cause of human morbidity and mortality, contributing to approximately 0.5 million deaths annually, with the potential for many more fatalities from recurring pandemic events. As IAV has the ability to become resistant to all major classes of influenza drugs,[1,2] additional antivirals that can target multiple drug-resistant forms of the virus are needed to support seasonal and pandemic preparedness.

The viral matrix protein 2 (M2) is required for IAV replication and is an established antiviral target. Among its multiple functions, M2 acts as a proton-gated channel that permits the flow of protons from acidifying endosomes into the virion core during entry. This in turn promotes hemagglutinin (HA)-mediated viral-host membrane fusion and release of viral RNA into the cytoplasm.[3] During virus assembly, M2 also recruits the matrix protein 1 (M1) to the assembly site and facilitates the budding of new virions by inducing host cell membrane curvature needed for scission.[4–7] Amantadine (*Amt*, **1**) and rimantadine (*Rmt*, **2**) (**Figure 1**) inhibit virus uncoating and assembly by acting directly on M2 proton conduction.[8–13] Resistance to these inhibitors arises from mutations in the M2 transmembrane domain, where over 95% of adamantane-resistant IAVs bear a serine-to-asparagine substitution at position 31 ($M2^{S31N}$), although substitutions like L26F, V27A, A30T, and G34E are also observed *in vitro* and/or in circulating viruses.[14]

After early work identified some potent *Amt*(**1**) analogs,[15] numerous analogs have been shown to inhibit $M2^{WT}$ and/or *Amt*(**1**)-resistant IAVs (mostly with $M2^{L26F}$ or $M2^{V27A}$).[16–22] For example, we described the antiviral activities of 57 synthetic *Amt*(**1**) analogs against (a) the drug-resistant A/H1N1/WSN/1933 virus containing $M2^{S31N}$; (b) an A/H1N1/WSN/1933 revertant

strain bearing an $M2^{WT}$ sequence (i.e., N31S); and/or (c) A/H1N1/WSN/1933-$M2^{WT}$ strains with additional *Amt*(**1**)-resistance markers like L26F, V27A, A30T, or G34E.[23] Of note, several of these compounds inhibited A/H1N1/WSN/1933 viruses containing $M2^{WT}$, $M2^{L26F}$, and/or $M2^{V27A}$ as well as the corresponding M2 proton currents in electrophysiology (EP) experiments. However, while none of these inhibited the unmodified A/H1N1/WSN/1933 strain bearing $M2^{S31N}$ nor $M2^{S31N}$-mediated proton currents,[19,22,23] some analogs could inhibit other IAV strains containing $M2^{S31N}$.[19,23] For instance, we found that compounds **38** and **49** (**Figure 1**) inhibited both A/H1N1/California/07/2009, containing $M2^{S31N}$, and A/H1N1/PR/8/1934, containing $M2^{A30T+S31N}$, at low micromolar concentrations despite no inhibition of their $M2^{S31N}$ proton currents.[19,23-33]

To date, the mechanisms by which *Amt*(**1**) analogs inhibit many $M2^{S31N}$-containing viruses without directly blocking $M2^{S31N}$ proton currents are poorly understood. For example, while some IAV inhibitors can act as lysosomotropic agents that inhibit viral-host membrane fusion by increasing endosomal pH,[24,25] the extent to which *Amt*(**1**) analogs employ this or other antiviral mechanisms has not been investigated. To address this question, we evaluated 36 *Amt*(**1**) analogs [23] against a panel of IAVs containing either $M2^{S31N}$ including A/H1N1/California/07/2009 (abbreviated here as A/CA/07/09^{S31N}), A/H1N1/PR/8/1934 (A/PR/$8/34^{S31N}$), A/H1N1/WS/1933 (A/WS/33^{S31N}) or $M2^{WT}$ including A/H3N2/Victoria/3/1975 (abbreviated here as A/Victoria/$3/75^{WT}$) and A2/H2N2/Taiwan/1/1964 (A2/Taiwan/$1/64^{WT}$). Selective analogs with low micromolar activity against one or more IAV with $M2^{S31N}$ were then characterized for their additional mechanisms of action and *in vivo* tolerability.

2. Materials and Methods

Detailed Materials and Methods can be found in Supporting Information.

3. Results

*3.1. Tested Amt(**1**) analogs*

Figure 1 shows structures of 36 assessed compounds. We tested memantine (**9**), cyclooctylamine (**10**), and **11-19** as *tert*-alkyl amine analogs of *Amt*(**1**). Compounds **25-28** are based on *Rmt*(**2**) with a linear alkyl, heterocyclic or carbocyclic substitution. Compounds **35-43, 46-47,** and **49-60** have an amino group at the C-2 position. Compounds **35-43** include an alkyl group at the C-2 adamantane carbon, **46** and **47** have a spirocyclopropyl moiety, **49-59** contain a spiropyrrolidine moiety, and **60** contains a spiropiperidine moiety.

3.2. Amt(**1**) *analogs inhibit both M2^{WT}- and M2^{S31N}-containing IAVs*

To elaborate on our previous observations that *Amt*(**1**) analogs such as **38** and **49** inhibit IAV without affecting the M2^{S31N} proton currents,[19,23] *Amt*(**1**) analogs were tested against a broader range of M2^{S31N} and M2^{WT} IAVs. M2^{S31N} viruses included A/CA/07/09^{S31N}, A/PR/8/34^{S31N} and A/WS/33^{S31N}, while M2^{WT} viruses included A/Victoria/3/75^{WT} and A2/Taiwan/1/64^{WT} (**Table 1**). Consistent with previous quantitative observations, [23] no microscopic evidence of cytotoxicity to MDCK cells was detected after 18 hours exposure at 50 μM or higher except for compound **27** which caused ~50% loss of cell viability at 20 but not 5 μM (data not shown). Using this approach, we found that *Rmt*(**2**) demonstrated strong activity against M2^{WT} viruses, with half-maximal effective concentration (EC_{50}) values of 0.5 μM and 1.6 μM against A/Victoria/3/75^{WT} and A2/Taiwan/1/64^{WT}, respectively (**Table 1**). Consistent with previous results,[19,34] *Rmt*(**2**) did not inhibit two M2^{S31N} viruses (EC_{50} = 106 and 314 μM against A/CA/07/09^{S31N} and A/WS/33^{S31N}, respectively), although it was active against A/PR/8/34^{S31N} (EC_{50} = 3.3 μM) despite the presence of M2$^{S31N+A30T}$.

Several *Amt*(**1**) analogs were also clearly active against $M2^{S31N}$ IAVs (**Table 1**). Against the A/CA/07/09^{S31N} virus, compounds **18**, **25-28**, **37-40, 42-43**, **49-55**, **57-58** and **60** exhibited high activity (defined here as an EC_{50} < 5 μM) or moderate activity (defined as an EC_{50} < 20 μM or ~5-fold lower than *Rmt*(**2**)), with **27** being the most active (EC_{50} = 0.8 μM, or 132-fold lower than *Rmt*(**2**)). Moderate activity against A/PR/8/34^{S31N} (*i.e.,* EC_{50} < 0.65 μM or 5-fold lower than *Rmt*(**2**)) was observed for compounds **28, 36, 38-40, 42** and **51**. When assessed against A/WS/33^{S31N}, compounds with EC_{50} < 65 μM (*i.e.,* 5-fold lower than *Rmt*(**2**)) included **15, 28, 36-40, 43, 51-52** and **59**. Overall, five compounds (**28, 38-40** and **51**) exhibited EC_{50} values at least 5-fold lower than *Rmt*(**2**) across all three $M2^{S31N}$ viruses (**Table 1**). Previous studies using EP showed that compounds **28** and **38** (as well as **35** and **49**) do not block proton currents of $M2^{S31N}$ from A/CA/07/09^{S31N}.[35]

In contrast, several *Amt*(**1**) analogs exhibited detectable activity (defined here as EC_{50} < 12.5 μM or within 25-fold of *Rmt*(**2**)) against the A/Victoria/3/75^{WT} IAV strain with $M2^{WT}$; these included **10**, **17-18**, **28**, **35-37**, **39**, **42**, **51**, **53**, and **56** (**Table 1**). Compounds **28**, **35-40**, **42-43**, **51**, and **59** also showed detectable activity against the A2/Taiwan/1/64^{WT} virus (*i.e.*, EC_{50} < 12.5 μM or within 25-fold of *Rmt*(**2**)) (**Table 1**). Consistent with these observations, compounds **28, 38,** and **51** inhibit proton currents from the $M2^{N31S}$-mutated proton channel of A/CA/07/09 (*i.e.,* reverted to WT).[35] However, contrary to observations with $M2^{S31N}$ viruses, where multiple analogs had at least 5-fold improvement over *Rmt*(**2**), no analog had this level of improvement over *Rmt*(**2**) except for compounds **42** and **43** against A2/Taiwan/1/64^{WT} (**Table 1**).

To determine whether *Amt*(**1**) analog activities were consistent across $M2^{S31N}$ and $M2^{WT}$ viruses, we performed linear regression analysis of the average EC_{50} for each compound across viruses (**Figure 2**). Notably, the EC_{50} values of all compounds tested against A/CA/07/09^{S31N} and A/PR/8/34^{S31N} which both contain $M2^{S31N}$, were well correlated (r^2 = 0.77;

$p < 0.0001$; **Figure 2A**). Significant correlations were also maintained between the EC_{50}s of A/CA/07/09^{S31N} and A/PR/8/34^{S31N} versus A/WS/33^{S31N}, which also has M2^{S31N} ($r^2 = 0.41$; $p = 0.013$ and $r^2 = 0.47$; $p = 0.009$, respectively; **Figure 2B-C**). These results suggest that *Amt*(**1**) analogs may act on the same viral and/or host target(s) in the context of these M2^{S31N} viruses. In contrast, no correlations were observed between M2^{S31N} and M2^{WT} viruses (all $r^2 < 0.13$; $p > 0.05$; **Figure 2D**), suggesting that the primary viral and/or host target(s) differ between these two groups. Similarly, no correlation was found between A/Victoria/3/75^{WT} and A2/Taiwan/1/64^{WT} (both M2^{WT}) (**Figure 2E**). The reason for the poor correlation between the two M2^{WT} viruses is not clear but could indicate additional virus-specific traits that might indirectly influence the activity of these analogs.

Based on these results, we selected a subset of analogs to characterize in greater detail as described below. We focused primarily on compound **38**, but also **49**, based on previous observations that they can inhibit viruses containing M2^{S31N} but do not immediately block M2^{S31N}-medicated proton currents in EP studies [19,35]. Compound **27** was chosen as it was the most active adamantyl amine against A/CA/07/09^{S31N}. Furthermore, **26**, **27**, **28** and **60** resembled **38** while bearing much bulkier adducts, while **39** represented the n-Bu analog of compound **38** (**Figure 1**).

3.3. Antiviral activity of Amt(***1***) *analogs is not due to inhibition of M2^{S31N}-dependent proton currents*

To rule out any direct effect on M2^{S31N} proton conduction, we used a previously-described whole-cell patch-clamp EP approach [27] with compound **38** representing analogs that inhibited all three M2^{S31N} viruses. Briefly, tsA-201 cells co-transfected with plasmids encoding GFP and M2^{S31N} (from A/CA/07/09^{S31N}) were held at a constant membrane potential of -40 mV,

and currents were recorded every 4 s by applying 100-ms pulses to -80 mV. Using this approach, we previously showed that robust, pH-dependent inward currents are readily inhibited with $M2^{WT}$ and $M2^{S31N}$-dependent inhibitors.[27] We then assessed the activity of **38** over a 30-minute exposure period. As shown in **Figure 3A**, single tsA-201 cells expressing $M2^{S31N}$ exhibited robust, low pH-dependent negative or inward current that decayed ~50% during continued exposure to low pH. This current could be maintained for more than 2400 seconds (40 minutes) and was inhibited approximately 25% with 100 μM *Amt*(**1**), consistent with previous results of its fast but limited inhibition.[27] However, when the same long-term procedure was done with 100 μM of **38**, no inhibition of $M2^{S31N}$ current was observed even after 2400 seconds (**Figure 3B**). The finding that compound **38** does not inhibit $M2^{S31N}$ currents even after prolonged exposure further argues against $M2^{S31N}$ channel inhibition as the mechanism underlying the activity of compound **38** and related compounds towards $M2^{S31N}$ viruses.

3.4. Antiviral activity of Amt*(**1**) analogs is not due to modulating endosomal pH*

In addition to inhibiting M2, some *Amt*(**1**) analogs can function as lysosomotropic agents, preventing viral-host membrane fusion by increasing endosomal pH.[24,25] Besides IAV, viruses like bovine papillomavirus (BPV) also rely on acidic endosomes for entry or uncoating within host cells. Compounds that elevate endosomal pH or disrupt the endocytosis process can inhibit BPV replication.[36] To explore whether *Amt*(**1**) analogs might modulate endosomal pH, we assessed compounds **27** and **38** in a miniplaque assay using BPV (P6 variant)-infected bovine embryonic kidney cells. While control agents chlorpromazine, ammonium chloride, chloroquine and bafilomycin A1 all inhibited BPV replication here (EC_{50}: 2.5, 0.4, 2.2 and 0.06 μM, respectively) at concentrations consistent with published results,[36] no inhibition was observed by up to 20 μM of either *Amt*(**1**) analog (**Figure 4**). No microscopic evidence of

209 cytotoxicity due to any compound, including **27**, was observed in uninfected bovine embryonic
210 kidney cells (data not shown). These results suggest that **27** and **38**, and presumably other
211 *Amt*(**1**) analogs, do not act as endosome neutralizers to inhibit $M2^{S31N}$ viruses.

212

213 *3.5. In vitro selection of* Amt*(**1**) analog-resistant viruses occurs through M2 mutations in $M2^{WT}$*
214 *but not $M2^{S31N}$ viruses*

215 To identify potential viral targets of these *Amt*(**1**) analogs, we conducted virus passaging
216 to select for compound-resistant viruses. MDCK cells were initially infected with A/H3N2/Hong
217 Kong/1/1968, which contains $M2^{WT}$, and passaged semi-weekly in the presence of 3.9 or 4.4
218 μM of compounds **27** or **38**, respectively (corresponding to 1 and 5 μg/mL). As anticipated, all
219 compounds induced rapid drug resistance. Following plaque purification and M-sequencing,
220 resistance was linked to known *Amt*(**1**)-resistance mutations in M2 including V27A for
221 compound **27** and A30T for **38** (**Table 2**). No resistance mutations were detected in infected
222 cells passaged in parallel in the absence of drugs. These results support that *Amt*(**1**) analogs
223 readily select for escape mutants bearing substitutions in M2, suggesting that, similar to *Amt*(**1**),
224 these analogs inhibit $M2^{WT}$ viruses by targeting M2 proton conduction.

225 We next used a subset of *Amt*(**1**) analogs for passaging experiments with an $M2^{S31N}$
226 virus. MDCK cells infected with A/CA/07/09^{S31N} were passaged semi-weekly in the presence of
227 5 μM of compound **38** or a triple combination of compounds **26**, **27** and **60**, each at 5 μM,
228 representing a diverse set of ring adducts at both C1 and C2 (**Table 3**). As an experimental
229 control, we performed parallel passaging of A/Victoria/3/75^{WT} virus with $M2^{WT}$ in the presence
230 of 50 μM *Amt*(**1**). In this control, drug resistance emerged after one passage: while the parent
231 virus had an EC_{50} value of 3.0 μM (n = 9) for *Amt*(**1**), passage #1 and #2 viruses were not

inhibited by *Amt*(**1**). In contrast, for A/CA/07/09^{S31N} grown under compound **38**, passages #1 to #5 remained fully sensitive (EC_{50} = 2.1 – 5.4 μM), but between passages #6 and #12, the virus became progressively resistant, with > 20-fold resistance by passage #10 onward (EC_{50} = 76 – 149 μM; **Table 3**). Similarly, the combination of **26**, **27** and **60** remained effective through 6 passages (EC_{50} = 1.0 – 1.2 μM) but developed ~6.6-fold resistance by passage #10 (EC_{50} = 7.9 μM; **Table 3**). Notably, the passage #12 virus resistant to compound **38** remained sensitive to compound **28,** with an EC_{50} of 10.2 μM only modestly increased compared to the parental virus (EC_{50} = 3.6 μM). Sequence analysis on the parental A/CA/07/09^{S31N} virus and passage #12 virus resistant to compound **38** indicated no differences in the region encoding M2 amino acids 10-73. Hence, resistance to **38** was not caused by additional mutations in M2 that underlie proton conduction.

Taken together, these results indicate *Amt*(**1**) analogs primarily act on M2 in viruses containing M2^{WT} but not M2^{S31N}. Additionally, since mutations selected during passaging viruses containing M2^{S31N} did not confer significant resistance across all *Amt*(**1**) analogs, it is likely that these analogs act on multiple and potentially overlapping viral targets.

3.6. Amt(**1**) *analogs inhibit the entry of M2^{S31N} virus in an HA and/or neuraminidase (NA)-dependent manner*

To determine whether *Amt*(**1**) analogs interfere with IAV's ability to infect MDCK cells, we first treated A/CA/07/09^{S31N} virus with or without 50 μM compound **38**. Virus-drug aliquots were then collected at 0, 1, 5-, 10-, 20- or 30-minute post-incubation and assessed for infectivity by miniplaque assay. At this stage, the final concentration of **38** was 0.5 μM, a concentration unlikely to inhibit virus growth (**Table 1**). After 5 minutes of incubation, IAV infectivity was

reduced by 46.7%; by 30 minutes, reduction reached 62.9% (**Figure 5**). These results suggest that **38** reduces virus infectivity before exposure to target cells.

To test whether **38** might act on HA and/or NA-mediated viral entry,[37] we next conducted an MDCK-based entry assay using murine leukemia virus-based pseudovirus bearing the HA and NA proteins of influenza A/Virginia/ATCC3/2009. As shown in **Figure 6**, *Amt*(**1**), *Rmt*(**2**), and compounds **26**, **49**, and **60** did not inhibit pseudovirus entry at 400 μM. In contrast, compound **38** exhibited clear activity, with an EC_{50} of 16 μM, followed by **39** and **28** with EC_{50}s of 29 and 64 μM, respectively. The EC_{50} of compound **38** was comparable to those of control viral entry inhibitors arbidol and hydroxychloroquine (**Figure 6**).

Taken together, these results indicate that a subset of analogs, exemplified by compound **38**, act on HA/NA-mediated vial entry and/or interfere with the ability of IAV to infect MDCK cells more generally.

3.7. Amt(**1**) *analogs impair M2-mediated M1 recruitment to the plasma membrane*

Six compounds evaluated above (**26, 28, 38, 39, 49, 60**) were next investigated for their ability to disrupt the intracellular distribution of the viral matrix proteins M1 and M2. HEK-293T cells were transfected with fluorescent constructs labelled with mEGFP and mCherry2, respectively, and their subcellular localization was monitored by fluorescence microscopy. HEK-293T cells were chosen due to their characteristic cell height, which makes it easier to find an optimal focal plane at the cell midplane and image the plasma membrane. In this context, we have also shown that M2 is essential for the proper recruitment of M1 to the plasma membrane (PM).[31] In cells lacking M2 expression (i.e., negative control, NC in **Figure 7**), M1 was uniformly distributed throughout the cytoplasm. Conversely, in the presence of M2 (positive control, PC in **Figure 7**), M1 was enriched at the PM, as expected.[54] Of note, treatment with 30

μM of *Amt*(**1**) analogs like compound **39** significantly decreased the number of cells with M1-PM association (**Figure 7; Figure S1**). Quantitative analysis indicated that all tested compounds significantly impaired M2-M1 interactions except for **38**, which only showed an approximately 10% reduction (**Figure 8**, **Table S1 and Figures S2-S3**). For instance, compound **39** reduced M2-M1 colocalization by approximately 63% (**Figures 7-8**).

Based on these mechanistic insights, the overall antiviral activity of *Amt*(**1**) analogs against $M2^{S31N}$ viruses arises from a combination of inhibitory effects on viral entry and disruption of M2-M1 colocalization.

3.8. Amt(**1**) *analogs and combinations are tolerated in vivo*

The ability of *Amt*(**1**) analogs to act on multiple aspects of IAV replication positions them as promising lead compounds for developing antivirals. These antivirals, in principle, could combine a direct effect on the $M2^{WT}$ channel with additional effects on viral entry and/or M2-M1 colocalization in $M2^{S31N}$-containing viruses. To evaluate *in vivo* safety, we conducted a pilot study comparing compounds **38** and **49** to *Amt*(**1**) for *in vivo* safety upon *i.p.* injection in CD-1 mice. All three compounds were tolerated at 30 mg/kg. However, compound **38** was uniformly lethal at 100 mg/kg, whereas **49** and *Amt*(**1**) were lethal at 300 mg/kg (**Table 4**). Furthermore, while **49** exhibited some signs of neurotoxicity at 30 mg/kg, no abnormalities were observed with either *Amt*(**1**) or **38** (**Table 4**). Hence, compound **38** is tolerated *in vivo* without neurotoxicity at least at 30 mg/kg.

4. Discussion

To effectively manage seasonal and pandemic IAV outbreaks and support vaccination efforts,[1,2,3] new antivirals are essential, particularly those capable of inhibiting drug-resistant

IAV strains. Drugs that target IAV through multiple mechanisms are preferable, as they are likely to provide a higher genetic barrier to resistance. Toward this goal, we evaluated the activities of 36 previously synthesized *Amt*(**1**) analogs against a panel of IAV strains containing either $M2^{WT}$ or *Amt*(**1**)-resistant $M2^{S31N}$. Notably, several compounds, including **15**, **18**, **25-28**, **36-43**, **49-55**, and **57-60**, inhibited up to three $M2^{S31N}$-containing viruses.

The activities of analogs to inhibit $M2^{S31N}$-containing viruses were well correlated (**Figure 2**), suggesting that they share at least some antiviral mechanisms, presumably by acting on the same viral and/or host targets. Using various molecular techniques, we identified and ruled out antiviral targets for a subset of analogs. As shown in **Table 5**, analogs had properties including ability to inhibit virus entry, achieved through inhibiting virus infectivity during pre-incubation before exposure to host cells, blocking H1N1 pseudovirus entry, and/or disrupting intracellular colocalization of M2 and M1, which is required for viral assembly and budding. We emphasize, however, that this range of antiviral activities observed here by these analogs is unlikely to be comprehensive. For example, in addition to inhibiting HA/NA-mediated pseudovirus entry, analogs like compound **38** may further antagonize viral entry by interfering with other viral proteins, mediating degradation of viral particles before infection, and/or inhibiting viral uncoating following entry. It is also possible that these activities could indirectly influence HA/NA-containing pseudovirus entry. Additional cellular processes required for virus replication may also be targeted by analogs; these could be identified and explored for example by global RNA sequencing approaches in uninfected cells. Subsequent studies with additional analogs and viruses with related replication cycles like influenza B, in addition to currently-circulating IAV strains, are warranted to dissect these mechanisms in greater detail and determine their impacts on IAV strains more generally.

Conversely, for some analogs, we demonstrated here and in previous studies [22,35] that virus inhibition did not correlate with inhibition of $M2^{S31N}$ proton currents, even when accounting for slow binding. For instance, compound **38** did not inhibit currents even after 2400 seconds of testing by EP. While it remains possible that a subset of *Amt*(**1**) analogs may possess a limited ability to inhibit $M2^{S31N}$ proton currents, the collective data argue that their primary antiviral targets likely lie elsewhere.

Our studies also indicate that some *Amt*(**1**) analogs do not act by modulating endosomal pH, unlike lysosomotropic agents. Lysosomotropic agents like chlorpromazine, ammonium chloride, chloroquine, and bafilomycin A1 inhibited BPV replication at low or sub-micromolar concentrations, whereas 20 μM of compounds **27** and **38** did not, although these observations have not been formally validated in an influenza model system. Notably, this lack of inhibition occurred despite the presence of hydrophobic adducts [38] in these analogs, which would be expected to accumulate in intracellular vesicles through membrane permeation by the electroneutral form and increase intravesicular pH.[30] For example, we recently observed that some IAVs like A/PR/8/34^{S31N} and A/CA/07/09^{S31N} are inhibited by *Amt*(**1**) analogs bearing different scaffold structures that subtly increase endosomal pH due to their basic character.[19,37] This increased endosomal pH, in turn, affects HA-mediated fusion, which requires low pH.[19,39] While our findings do not rule out this mechanism for all *Amt*(**1**) analogs assessed here, they further support the existence of additional antiviral mechanisms of action.

In virus passaging experiments, we observed that $M2^{WT}$ viruses readily developed resistance against *Amt*(**1**) analogs by acquiring V27A or A30T mutations in M2. However, using the A/CA/07/09^{S31N} with $M2^{S31N}$, we showed that resistance to compound **38** occurred between passages 6 and 12. Similarly, the combination of **26**, **27**, and **60** remained effective through 6 passages. Notably, no additional mutations in M2 were detected in these *Amt*(**1**)-resistant

viruses, further supporting the presence of other antiviral targets. However, comprehensive virus-wide genome sequencing, obtained from additional cultures, is needed to identify potential resistance mutations such as those that may arise in HA.[19] The delayed emergence of resistance in virus with $M2^{S31N}$, compared to the rapid resistance seen in the $M2^{WT}$ virus, suggests that IAV is less capable of overcoming targeting of these alternative antiviral mechanisms. Interestingly, viruses which generated resistance to the combination of compounds **26**, **27**, and **60** retained sensitivity to compound **38**, further supporting that analogs are likely to act on multiple and perhaps complementary antiviral targets (**Table 5**). Consequently, the development of *Amt*(**1**)-derived monotherapies or combination therapies optimized against several viral targets, including those identified here (i.e., virus entry and M2-M1 association), reversion of $M2^{S31N}$ to $M2^{WT}$, and potential increases in endosomal pH, may provide a particularly high genetic barrier to future IAV drug resistance.

Notably, different *Amt*(**1**) analogs exhibited a spectrum of overlapping activities. Some were more effective at blocking viral entry, while others excelled at disrupting M2-M1 interactions (**Table 5**). These differences align with our observations that IAV resistant to compounds **26**, **27**, and **60** retain sensitivity to compound **38**. We observed that compound **38** could directly inhibit virus entry, with 50 μM reducing virus entry by ~50% after just 5 minutes of pre-incubation. Furthermore, compound **38**, unlike compounds **26** and **60**, inhibited H1N1 pseudovirus entry with an EC_{50} of 16 μM. Our previous studies of compound **38** suggest that HA can be a target in some $M2^{S31N}$ viruses such as $A/CA/07/09^{S31N}$.[19] This may be driven by amino acid variants in HA that affect its binding to cell receptors and/or the efficiency of HA conformational changes at low pH [19]. It was also reported that $A/PR/8/34^{S31N}$ is particularly sensitive to increases in endosomal pH caused by the intrinsic basic properties (*i.e.*, alkaline pH-inducing) of *Amt*(**1**) analogs bearing lipophilic scaffold structures.[37] Conversely, compounds

26, **60**, and others are more effective at disrupting M2-M1 colocalization compared to compound **38**. This is significant as impairment of M1 recruitment to the PM affects viral particle production.[40,41] However, we have not yet explored whether these *Amt*(**1**) analogs can inhibit other aspects of M1 activity such as during viral entry when M1 dissociates from ribonucleoproteins, allowing them to enter the nucleus. Thus, intraviral buffering that inhibits M1-RNP disruption could be an additional mechanism of action worth investigating.

The structural changes in these *Amt*(**1**)-analogs, though often subtle, resulted in different activities in blocking virus entry and disrupting M2-M1 colocalization. Most *Amt*(**1**) analogs that perturb M2-M1 colocalization have lipophilic adducts attached at the 1- or 2-adamantyl position. These include 2-(1-adamantyl)piperidine (**26**), 1-adamantyl-1-cyclopentylamine (**27**), 1-adamantyl-1-cyclohexylamine (**28**), 2-n-butyl-2-adamantylamine (**39**) and the spiranic pyrrolidine (**49**) and spirnanic piperidine (**60**). However, while the heterocyclic or carbocyclic amines **26-28, 49, 60,** and **39** inhibit M2-M1 colocalization, 2-n-propyl-2-adamantylamine (**38**), which also bears an alkyl adduct like **39**, did not. Interestingly, **26-28,** and **39** have higher lipophilicity compared to compound **38** (**Table S2**).

Further support for the relevance of these M2-independent antiviral targets in future therapeutic development comes from a preliminary toxicity study in mice, where compound **38** and, to an extent, **49** were tolerated at 30 mg/kg. Although these compounds were lethal at higher concentrations, indicating narrower therapeutic windows than *Amt*(**1**) which was tolerated at 100 mg/kg, these results indicate that future *in vivo* measures of these analogs are feasible and support further evaluation of optimized *Amt*(**1**) analogs for absorption, distribution, metabolism, excretion and pharmacokinetics (ADME-PK) as well as *in vivo* efficacy studies.

5. Conclusion

In summary, we present a reference study for a series of *Amt*(**1**) variants against various IAV strains and their antiviral mechanisms. We show that some *Amt*(**1**) analogs exhibit low micromolar activities against three $M2^{S31N}$-containing viruses. Specifically, we observed that the 2-propyl-2-adamantyl analog **38** inhibits virus cellular entry, while others like the 1-adamantyl substituted piperidine analog **49** and the 2-adamantyl substituted spiranic pyrrolidine analog **26** disrupt M2-M1 colocalization required for intracellular viral assembly and budding. These patterns of antiviral activities, combined with *in vivo* tolerance of selected analogs, highlight the potential of developing optimized *Amt*(**1**) analogs or combination therapies with higher barriers to drug resistance.

6. Abbreviations

ADME-PK, absorption, distribution, metabolism, excretion and pharmacokinetics; Amt, amantadine; EC_{50}, half-maximal effective concentration; EP, electrophysiology; HA, hemagglutinin; IAV, influenza A virus; M1, viral matrix protein 1; M2, viral matrix protein 2; NA, neuraminidase; PC, positive control; PM, plasma membrane; Rmt, rimantadine. Virus abbreviations: $A/CA/07/09^{S31N}$, A/H1N1/California/07/2009 virus with $M2^{S31N}$; $A/PR/8/34^{S31N}$, A/H1N1/PR/8/1934 virus with $M2^{A30T+S31N}$; $A/WS/33^{S31N}$, A/H1N1/WS/1933 virus with $M2^{S31N}$; $A/Victoria/3/75^{WT}$, A/H3N2/Victoria/3/1975 virus with $M2^{WT}$; $A2/Taiwan/1/64^{WT}$, A2/H2N2/Taiwan/1/1964 virus with $M2^{WT}$.

7. Acknowledgements

We thank Chiesi Hellas for supporting this research (SARG No 10354), and Professor Nikolas Kolokouris (NKUA) for providing samples of compounds **46** and **47**. The authors thank Dr. Donald Smee for providing Influenza A/H1N1/California/07/2009.

8. Author contributions

Conceptualization: A.G., A.K.; Formal analysis: F.B.J., D.C.K.; Funding acquisition: S.C., D.F., I.T.; Investigation: I.V.A., F.B.J., D.C.K., C.M., L.N., A.P., M.R., F.X.S., C.T., I.T., R.Z.; Methodology: S.C., D.F., F.B.J., A.K., D.C.K., L.N., F.X.S.; Supervision: S.C., D.F., A.K., L.N., F.X.S., I.T.; Writing – original draft: A.K., I.T.; Writing – review and editing: S.C., A.K., L.N., A.P., I.T.

9. Funding sources

Funding was provided by the Natural Sciences and Engineering Research Council of Canada (grant number RGPIN-2022-03021; to D.F.) and Canadian Institutes of Health Research Project Grants (grant number PJT-175024 to D.F. and PJT-153058 to I.T.) and the German Research Foundation (grant number #254850309 to S.C.). Miniplaque shell vial assays were funded by MicroVir Laboratories (Orem, UT, USA). The funders had no role in study design, data collection and analysis, decision to publish, or preparation of the manuscript.

10. References

(1) Javanian, M.; Barary, M.; Ghebrehewet, S.; Koppolu, V.; Vasigala, V.; Ebrahimpour, S. A Brief Review of Influenza Virus Infection. *J Med Virol* **2021**, *93* (8), 4638–4646. https://doi.org/10.1002/jmv.26990.

(2) Jones, J. C.; Yen, H.-L.; Adams, P.; Armstrong, K.; Govorkova, E. A. Influenza Antivirals and Their Role in Pandemic Preparedness. *Antiviral Res* **2023**, *210*, 105499. https://doi.org/10.1016/j.antiviral.2022.105499.

(3) Jalily, P. H.; Duncan, M. C.; Fedida, D.; Wang, J.; Tietjen, I. Put a Cork in It: Plugging the M2 Viral Ion Channel to Sink Influenza. *Antiviral Res* **2020**, *178*, 104780. https://doi.org/10.1016/j.antiviral.2020.104780.

(4) Rossman, J. S.; Jing, X.; Leser, G. P.; Balannik, V.; Pinto, L. H.; Lamb, R. A. Influenza Virus M2 Ion Channel Protein Is Necessary for Filamentous Virion Formation. *J Virol* **2010**, *84* (10), 5078–5088. https://doi.org/10.1128/JVI.00119-10.

(5) Rossman, J. S.; Jing, X.; Leser, G. P.; Lamb, R. A. Influenza Virus M2 Protein Mediates ESCRT-Independent Membrane Scission. *Cell* **2010**, *142* (6), 902–913. https://doi.org/10.1016/j.cell.2010.08.029.

(6) Chen, B. J.; Lamb, R. A. Mechanisms for Enveloped Virus Budding: Can Some Viruses Do without an ESCRT? *Virology* **2008**, *372* (2), 221–232. https://doi.org/10.1016/j.virol.2007.11.008.

(7) Rossman, J. S.; Lamb, R. A. Influenza Virus Assembly and Budding. *Virology* **2011**, *411* (2), 229–236. https://doi.org/10.1016/j.virol.2010.12.003.

(8) Cady, S. D.; Schmidt-Rohr, K.; Wang, J.; Soto, C. S.; DeGrado, W. F.; Hong, M. Structure of the Amantadine Binding Site of Influenza M2 Proton Channels in Lipid Bilayers. *Nature* **2010**, *463* (7281), 689–692. https://doi.org/10.1038/nature08722.

(9) Wright, A. K.; Batsomboon, P.; Dai, J.; Hung, I.; Zhou, H. X.; Dudley, G. B.; Cross, T. A. Differential Binding of Rimantadine Enantiomers to Influenza A M2 Proton Channel. *J Am Chem Soc* **2016**, *138* (5), 1506–1509. https://doi.org/10.1021/jacs.5b13129.

(10) Ma, C.; Polishchuk, A. L.; Ohigashi, Y.; Stouffer, A. L.; Schon, A.; Magavern, E.; Jing, X.; Lear, J. D.; Freire, E.; Lamb, R. A.; DeGrado, W. F.; Pinto, L. H. Identification of the Functional Core of the Influenza A Virus A/M2 Proton-Selective Ion Channel. *Proc Natl Acad Sci U S A* **2009**, *106* (30), 12283–12288. https://doi.org/0905726106 [pii]\r10.1073/pnas.0905726106 [doi].

(11) Thomaston, J. L.; Polizzi, N. F.; Konstantinidi, A.; Wang, J.; Kolocouris, A.; Degrado, W. F. Inhibitors of the M2 Proton Channel Engage and Disrupt Transmembrane Networks of Hydrogen-Bonded Waters. *J Am Chem Soc* **2018**, *140* (45), 15219–15226. https://doi.org/10.1021/jacs.8b06741.

(12) Thomaston, J. L.; Konstantinidi, A.; Liu, L.; Lambrinidis, G.; Tan, J.; Caffrey, M.; Wang, J.; Degrado, W. F.; Kolocouris, A. X-Ray Crystal Structures of the Influenza M2 Proton Channel Drug-Resistant V27A Mutant Bound to a Spiro-Adamantyl Amine Inhibitor Reveal the Mechanism of Adamantane Resistance. *Biochemistry* **2020**, *59* (4), 627–634. https://doi.org/10.1021/acs.biochem.9b00971.

(13) Andreas, L. B.; Barnes, A. B.; Corzilius, B.; Chou, J. J.; Miller, E. A.; Caporini, M.; Rosay, M.; Griffin, R. G. Dynamic Nuclear Polarization Study of Inhibitor Binding to the M2 18–60 Proton Transporter from Influenza A. *Biochemistry* **2013**, *52* (16), 2774–2782. https://doi.org/10.1021/bi400150x.

(14) Dong, G.; Peng, C.; Luo, J.; Wang, C.; Han, L.; Wu, B.; Ji, G.; He, H. Adamantane-Resistant Influenza a Viruses in the World (1902-2013): Frequency and Distribution of

M2 Gene Mutations. *PLoS One* **2015**, *10* (3), 1–20. https://doi.org/10.1371/journal.pone.0119115.

(15) Aldrich, P. E.; Hermann, E. C.; Meier, W. E.; Paulshock, M.; Prichard, W. W.; Snyder, J. A.; Watts, J. C. Antiviral Agents. 2. Structure-Activity Relationships of Compounds Related to 1-Adamantanamine. *J Med Chem* **1971**, *14* (6), 535–543. https://doi.org/10.1021/jm00288a019.

(16) Kolocouris, N.; Foscolos, G. B.; Kolocouris, A.; Marakos, P.; Pouli, N.; Fytas, G.; Ikeda, S.; De Clercq, E. Synthesis and Antiviral Activity Evaluation of Some Aminoadamantane Derivatives. *J Med Chem* **1994**, *37* (18), 2896–2902. https://doi.org/10.1021/jm00044a010.

(17) Stamatiou, G.; Foscolos, G. B.; Fytas, G.; Kolocouris, A.; Kolocouris, N.; Pannecouque, C.; Witvrouw, M.; Padalko, E.; Neyts, J.; Clercq, E. D. Heterocyclic Rimantadine Analogues with Antiviral Activity. *Bioorg Med Chem* **2003**, *11* (24). https://doi.org/10.1016/j.bmc.2003.09.024.

(18) Zoidis, G.; Kolocouris, N.; Foscolos, G. B.; Kolocouris, A.; Fytas, G.; Karayannis, P.; Padalko, E.; Neyts, J.; De Clercq, E. Are the 2-Isomers of the Drug Rimantadine Active Anti-Influenza A Agents? *Antivir Chem Chemother* **2003**, *14* (3).

(19) Kolocouris, A.; Tzitzoglaki, C.; Johnson, F. B.; Zell, R.; Wright, A. K.; Cross, T. A.; Tietjen, I.; Fedida, D.; Busath, D. D. Aminoadamantanes with Persistent in Vitro Efficacy against H1N1 (2009) Influenza A. *J Med Chem* **2014**, *57* (11), 4629–4639. https://doi.org/10.1021/jm500598u.

(20) Balannik, V.; Carnevale, V.; Fiorin, G.; Levine, B. G.; Lamb, R. A.; Klein, M. L.; DeGrado, W. F.; Pinto, L. H. Functional Studies and Modeling of Pore-Lining Residue Mutants of the Influenza A Virus M2 Ion Channel. *Biochemistry* **2010**, *49* (4), 696–708. https://doi.org/10.1021/bi901799k.

(21) Wang, J.; Ma, C.; Balannik, V.; Pinto, L. H.; Lamb, R. A.; Degrado, W. F. Exploring the Requirements for the Hydrophobic Scaffold and Polar Amine in Inhibitors of M2 from Influenza A Virus. *ACS Med Chem Lett* **2011**, *2* (4), 307–312. https://doi.org/10.1021/ml100297w.

(22) Drakopoulos, A.; Tzitzoglaki, C.; McGuire, K.; Hoffmann, A.; Ma, C.; Freudenberger, K.; Konstantinidi, A.; Kolocouris, D.; Hutterer, J.; Gauglitz, G.; Wang, J.; Schmidtke, M.; Busath, D. D.; Kolocouris, A.; Kolokouris, D.; Ma, C.; Freudenberger, K.; Hutterer, J.; Gauglitz, G.; Wang, J.; Schmidtke, M.; Busath, D. D.; Kolocouris, A. Unraveling the Binding, Proton Blockage, and Inhibition of Influenza M2 WT and S31N by Rimantadine Variants. *ACS Med Chem Lett* **2018**, *9* (3), 198–203. https://doi.org/10.1021/acsmedchemlett.7b00458.

(23) Stampolaki, M.; Hoffmann, A.; Tekwani, K.; Georgiou, K.; Tzitzoglaki, C.; Ma, C.; Becker, S.; Schmerer, P.; Döring, K.; Stylianakis, I.; Turcu, A. L.; Wang, J.; Vázquez, S.; Andreas, L. B.; Schmidtke, M.; Kolocouris, A. A Study of the Activity of Adamantyl

Amines against Mutant Influenza A M2 Channels Identified a Polycyclic Cage Amine Triple Blocker, Explored by Molecular Dynamics Simulations and Solid-State NMR**. *ChemMedChem* **2023**. https://doi.org/10.1002/cmdc.202300182.

(24) Chen, H.-W.; Cheng, J. X.; Liu, M.-T.; King, K.; Peng, J.-Y.; Zhang, X.-Q.; Wang, C.-H.; Shresta, S.; Schooley, R. T.; Liu, Y.-T. Inhibitory and Combinatorial Effect of Diphyllin, a v-ATPase Blocker, on Influenza Viruses. *Antiviral Res* **2013**, *99* (3), 371–382. https://doi.org/10.1016/j.antiviral.2013.06.014.

(25) Jang, Y.; Shin, J. S.; Yoon, Y.-S.; Go, Y. Y.; Lee, H. W.; Kwon, O. S.; Park, S.; Park, M.-S.; Kim, M. Salinomycin Inhibits Influenza Virus Infection by Disrupting Endosomal Acidification and Viral Matrix Protein 2 Function. *J Virol* **2018**, *92* (24). https://doi.org/10.1128/JVI.01441-18.

(26) Laporte, M.; Stevaert, A.; Raeymaekers, V.; Boogaerts, T.; Nehlmeier, I.; Chiu, W.; Benkheil, M.; Vanaudenaerde, B.; Pöhlmann, S.; Naesens, L. Hemagglutinin Cleavability, Acid Stability, and Temperature Dependence Optimize Influenza B Virus for Replication in Human Airways. *J Virol* **2019**, *94* (1). https://doi.org/10.1128/JVI.01430-19.

(27) Jalily, P. H.; Eldstrom, J.; Miller, S. C.; Kwan, D. C.; Tai, S. S.-H.; Chou, D.; Niikura, M.; Tietjen, I.; Fedida, D. Mechanisms of Action of Novel Influenza A/M2 Viroporin Inhibitors Derived from Hexamethylene Amiloride. *Mol Pharmacol* **2016**, *90* (2), 80–95. https://doi.org/10.1124/mol.115.102731.

(28) Hintermann, B.; Knupp, M.; Barg, A. Supramalleolar Osteotomies for the Treatment of Ankle Arthritis. *J Am Acad Orthop Surg* **2016**, *24* (7), 424–432. https://doi.org/10.5435/JAAOS-D-12-00124.

(29) Appleyard, G. Amantadine Resistance as a Genetic Marker for Influenza Viruses. *Journal of General Virology* **1977**, *36* (2), 249–255. https://doi.org/10.1099/0022-1317-36-2-249.

(30) Scholtissek, C.; Quack, G.; Klenk, H. D.; Webster, R. G. How to Overcome Resistance of Influenza A Viruses against Adamantane Derivatives. *Antiviral Res* **1998**, *37*, 83–95. https://doi.org/10.1016/S0166-3542(97)00061-2.

(31) Petrich, A.; Dunsing, V.; Bobone, S.; Chiantia, S. Influenza A M2 Recruits M1 to the Plasma Membrane: A Fluorescence Fluctuation Microscopy Study. *Biophys J* **2021**, *120* (24), 5478–5490. https://doi.org/10.1016/j.bpj.2021.11.023.

(32) Petrich, A.; Dunsing, V.; Bobone, S.; Chiantia, S. Influenza A M2 Recruits M1 to the Plasma Membrane: A Fluorescence Fluctuation Microscopy Study. *Biophys J* **2021**, *120* (24), 5478–5490. https://doi.org/10.1016/j.bpj.2021.11.023.

(33) Mathiasen, J. R.; Moser, V. C. The Irwin Test and Functional Observational Battery (FOB) for Assessing the Effects of Compounds on Behavior, Physiology, and Safety

Pharmacology in Rodents. *Curr Protoc Pharmacol* **2018**, *83* (1), e43. https://doi.org/10.1002/cpph.43.

(34) Torres, E.; Fernández, R.; Miquet, S.; Font-Bardia, M.; Vanderlinden, E.; Naesens, L.; Vázquez, S. Synthesis and Anti-Influenza a Virus Activity of 2,2-Dialkylamantadines and Related Compounds. *ACS Med Chem Lett* **2012**, *3* (12), 1065–1069. https://doi.org/10.1021/ml300279b.

(35) Tzitzoglaki, C.; Wright, A.; Freudenberger, K.; Hoffmann, A.; Tietjen, I.; Stylianakis, I.; Kolarov, F.; Fedida, D.; Schmidtke, M.; Gauglitz, G.; Cross, T. A.; Kolocouris, A. Binding and Proton Blockage by Amantadine Variants of the Influenza M2WT and M2S31N Explained. *J Med Chem* **2017**, *60* (5), 1716–1733. https://doi.org/10.1021/acs.jmedchem.6b01115.

(36) Day, P. M.; Lowy, D. R.; Schiller, J. T. Papillomaviruses Infect Cells via a Clathrin-Dependent Pathway. *Virology* **2003**, *307* (1), 1–11. https://doi.org/10.1016/s0042-6822(02)00143-5.

(37) Torres, E.; Duque, M. D.; Vanderlinden, E.; Ma, C.; Pinto, L. H.; Camps, P.; Froeyen, M.; Vázquez, S.; Naesens, L. Role of the Viral Hemagglutinin in the Anti-Influenza Virus Activity of Newly Synthesized Polycyclic Amine Compounds. *Antiviral Res* **2013**, *99* (3), 281–291. https://doi.org/10.1016/j.antiviral.2013.06.006.

(38) Pisonero-Vaquero, S.; Medina, D. L. Lysosomotropic Drugs: Pharmacological Tools to Study Lysosomal Function. *Curr Drug Metab* **2017**, *18* (12), 1147–1158. https://doi.org/10.2174/1389200218666170925125940.

(39) Daniels, R. Fusion Mutants of the Influenza Virus Hemagglutinin Glycoprotein. *Cell* **1985**, *40* (2), 431–439. https://doi.org/10.1016/0092-8674(85)90157-6.

(40) Wang, D.; Harmon, A.; Jin, J.; Francis, D. H.; Christopher-Hennings, J.; Nelson, E.; Montelaro, R. C.; Li, F. The Lack of an Inherent Membrane Targeting Signal Is Responsible for the Failure of the Matrix (M1) Protein of Influenza A Virus To Bud into Virus-Like Particles. *J Virol* **2010**, *84* (9), 4673–4681. https://doi.org/10.1128/JVI.02306-09.

(41) Liu, H.; Grantham, M. L.; Pekosz, A. Mutations in the Influenza A Virus M1 Protein Enhance Virus Budding To Complement Lethal Mutations in the M2 Cytoplasmic Tail. *J Virol* **2018**, *92* (1). https://doi.org/10.1128/JVI.00858-17.

(42) Chen, B. J.; Leser, G. P.; Jackson, D.; Lamb, R. A. The Influenza Virus M2 Protein Cytoplasmic Tail Interacts with the M1 Protein and Influences Virus Assembly at the Site of Virus Budding. *J Virol* **2008**, *82* (20), 10059–10070. https://doi.org/10.1128/jvi.01184-08.

598 **11. Supporting Information**

599 Detailed Materials and Methods

600 Table S1, S2

601 Figure S1-S3

602

Table 1. Ar[illegible] values were obtained from mini-plaque testing for dose-response or single-dose screens, using cultured MDCK cells, based on least-squares fitting of single-site binding curves. Values in bold reflect EC_{50}s > 5-fold below the EC_{50} of *Rmt*(**2**). Underlined values denote EC_{50}s < 5 μM for $M2^{S31N}$ viruses. n.t., not tested.

	EC_{50} (μM)				
Compound	A/CA/07/09^{S31N}	A/PR/8/34^{S31N}	A/WS/33^{S31N}	A/Victoria/3/75^{WT}	A2/Taiwan/1/64^{WT}
Rmt(**2**)	106 ± 41	3.3 ± 0.5	314 ± 135	0.5 ± 0.1	1.6 ± 0.3
9	70.8 ± 10.5	n.t.	n.t.	72.2 ± 10.6	n.t.
10	363 ± 3.8	n.t.	n.t.	10.2 ± 2.6	n.t.
11	61.2 ± 6.6	n.t.	n.t.	39.0 ± 4.5	n.t.
12	41.9 ± 11.8	n.t.	n.t.	91.0 ± 1.5	n.t.
14	241 ± 121	n.t.	n.t.	105 ± 35.0	n.t.
15	43.2 ± 1.1	0.8 ± 0.8	**37.4 ± 11.8**	33.9 ± 7.3	n.t.
16	293 ± 273	n.t.	n.t.	21.7 ± 2.2	n.t.
17	340 ± 231	n.t.	n.t.	11.9 ± 2.3	n.t.
18	**11.7 ± 1.0**	n.t.	n.t.	3.8 ± 0.4	n.t.
19	398 ± 176	n.t.	n.t.	43.6 ± 6.1	n.t.
25	**15.4 ± 2.4**	n.t.	n.t.	n.t.	n.t.
26	**7.0 ± 1.2**	n.t.	n.t.	n.t.	n.t.
27	**0.8 ± 0.1**	n.t.	n.t.	n.t.	n.t.
28	**3.6 ± 0.5**	**0.3 ± 0.5**	**53.7 ± 11.5**	2.3 ± 0.4	4.2 ± 1.0
35	151 ± 33.0 [19]	3.8 ± 1.0	112 ± 14.8	3.3 ± 0. 9	0.8 ± 0.3

36	53.9 ± 12.6 [19]	**0.4 ± 0.4**	**18.7 ± 4.5**	2.0 ± 0.4	0.5 ± 0.5
37	**19.0 ± 3.0** [19]	1.8 ± 0.9	**22.5 ± 2.9**	2.0 ± 0.4	0.8 ± 0.3
38	**4.7 ± 0.9** [19]	**0.5 ± 0.2**	**37.6 ± 8.4**	23.4 ± 7.6	0.5 ± 0.5
39	**7.4 ± 0.9** [19]	**0.3 ± 0.5**	**34.6 ± 4.1**	4.0 ± 1.2	1.5 ± 0.2
40	**5.8 ± 0.4** [19]	**0.3 ± 0.5**	**20.5 ± 3.7**	13.3 ± 2.0	0.4 ± 0.1
42	**17.4 ± 1.4** [19]	**0.3 ± 0.5**	86.0 ± 19.6	5.2 ± 1.0	**0.2 ± 0.2**
43	**9.7 ± 1.4** [19]	1.2 ± 1.1	**26.9 ± 14.5**	17 ± 3.1	**0.2 ± 0.3**
46	399 ± 297	n.t.	n.t.	n.t.	n.t.
47	30.8 ± 49.0	n.t.	n.t.	n.t.	n.t.
49	**8.1 ± 2.1**	n.t.	n.t.	n.t.	n.t.
50	**7.9 ± 1.5**	n.t.	n.t.	n.t.	n.t.
51	**2.7 ± 0.3**	**0.3 ± 0.5**	**34.2 ± 8.4**	0.6 ± 0.2	0.5 ± 0.2
52	**7.2 ± 2.0**	n.t.	**9.6 ± 1.4**	55.3 ± 0.5	n.t.
53	**10.2 ± 1.2**	0.8 ± 0.8	n.t.	5.7 ± 1.8	n.t.
54	**9.5 ± 1.6**	n.t.	n.t.	19.2 ± 3.5	n.t.
55	**7.0 ± 0.8**	n.t.	n.t.	58.3 ± 11.5	n.t.
56	34.2 ± 4.4	n.t.	n.t.	3.2 ± 2.0	n.t.
57	**7.7 ± 2.0**	n.t.	n.t.	16.2 ± 7.5	n.t.
58	**8.7 ± 1.7**	n.t.	n.t.	38.5 ± 1.0	n.t.
59	34.1 ± 1.2	0.7 ± 0.5	**14.9 ± 1.6**	34.1 ± 7.9	1.2 ± 0.2
60	**19.8 ± 17.1**	n.t.	n.t.	n.t.	n.t.

603

604 **Table 2.** Mutations developed influenza $M2^{WT}$ after passaging experiments with compounds **27**

605 or **38**.

A/H3N2/Hong Kong/1/1968 ($M2^{WT}$)	**Compound**	**27**	**38**
Passage number	**Plaque number** [a]	**3.9 µM**	**4.4 µM**
2	**1**	V27A	A30T
	2	V27A	A30T
	3	V27A	A30T
5	**1**	V27A	A30T
	2	V27A	A30T
	3	V27A	A30T
			5 µg/ml
10	**1**		A30T
	2		A30T
	3		A30T

606 [a] Three separate plaques were sampled and sequenced at passages 2, 5, and/or 10.

607 **Table 3.** Resistance testing of amantadine (**1**) variants against an amantadine-sensitive H3N2
608 virus and potent amantadine variants against amantadine-resistant H1N1 (2009).

	1 (5 μM)	**38 (**5 μM)	**26, 27, 60 (**5 μM)
	A/Victoria/3/75^{WT}	A/CA/07/09^{S31N}	A/CA/07/09^{S31N}
Passage #	EC_{50} ± S.E. (μM)	EC_{50} ± S.E. (μM)	EC_{50} ± S.E. (μM)
0	2.8 ± 0.3	4.7 ± 0.9	1.0 ± 0.2
1	> 50	5.4 ± 1.4	
2	> 50	3.7 ± 0.5	
5		2.1 ± 1.6	
6			1.2 ± 0.1
8		18.5 ± 1.0	
10		76 ± 9	7.9 ± 0.8
12		149 ± 115	
Compound **28**		10.2 ±1.7	

609

610 **Table 4**. *In vivo* toxicity from intraperitoneal infections of *Amt*(**1**) and compounds **38** and **49**.

611

Dose (mg/kg)	*Amt*(**1**)	Compound **38**	Compound **49**
30	0 (2:2) [a]	0 (1:2)	0 (2:1) [b]
100	0 (2:1) [c]	3 (2:1)	2 (3:1) [d]
300	3 (2:1)	N.D.	3 (2:1)

612

613

614

615

616 [a] Number of deaths within 48 hours (number of males injected: number of females injected). [b]
617 Neurotoxicity observed including slightly abnormal gate, quivers, and hyper-responsiveness to
618 touch and noise. [c] Moderate trembling or quivers observed. [d] Ataxic gait, moderately abnormal
619 gait, slightly or somewhat impaired mobility, mild tremors, motor incoordination observed.

620 **Table 5.** Summary of bioactivities of select *Amt*(**1**) analogs. *, compounds passaged in

621 combination.

Compound	Inhibits $M2^{S31N}$ by EP at 100 µM	Inhibits BPV replication (lysosomotropic effect) at 20 µM	Mutations in $M2^{WT}$ develop at 1-5 µg/mL	Mutations in $M2^{S31N}$ develop at 5 µM	Inhibits cellular entry of IAV with $M2^{S31N}$ at 5 µM	H1N1 pseudovirus entry (EC_{50}, µM)	Inhibits M1-$M2^{S31N}$ colocalization at 30 µM	Tolerated *in vivo* at 30 mg/kg
26				No*		> 400	Yes	
27		No	V27A	No*			Yes	
28	No [31]					64	Yes	
38	No	No	A30T	No	Yes, at 50 µM	16	No	Yes
39						29	Yes	
49	No [31]					> 400	Yes	Yes
60				No*		> 400	Yes	

622

623

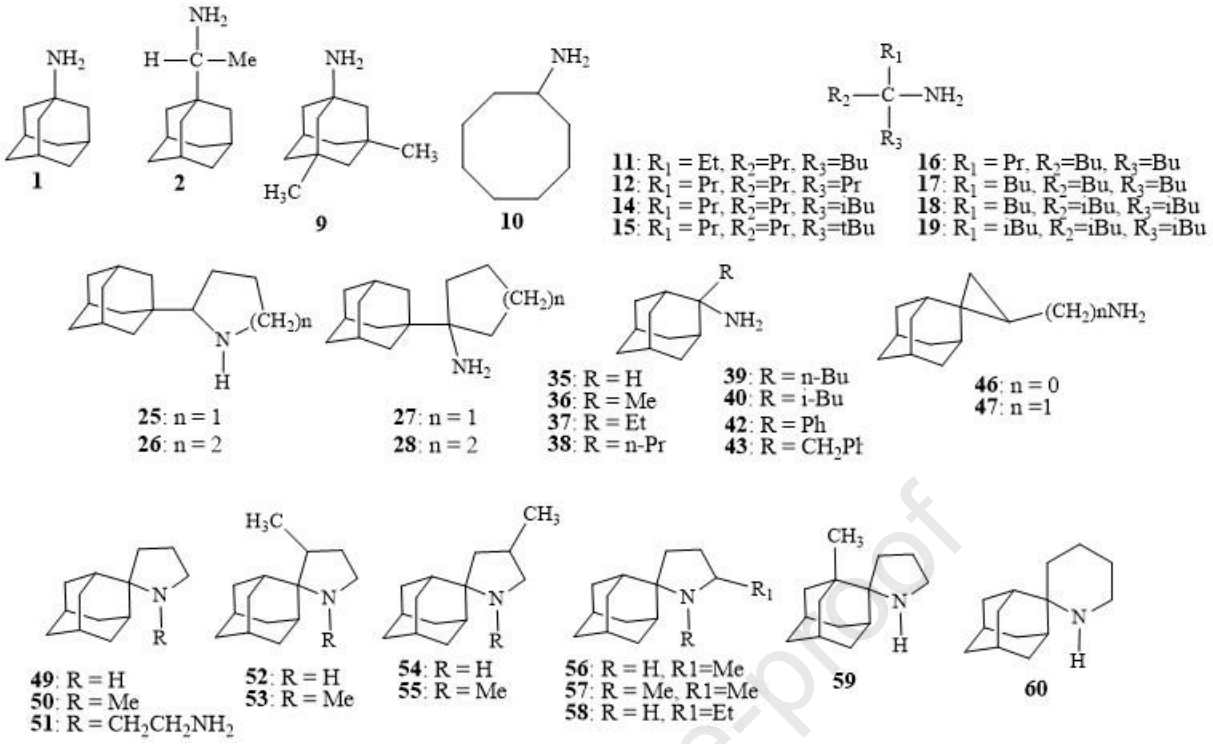

Figure 1. Chemical structures of *Amt*(**1**) analogs tested against $M2^{WT}$ and $M2^{S31N}$ IAV.

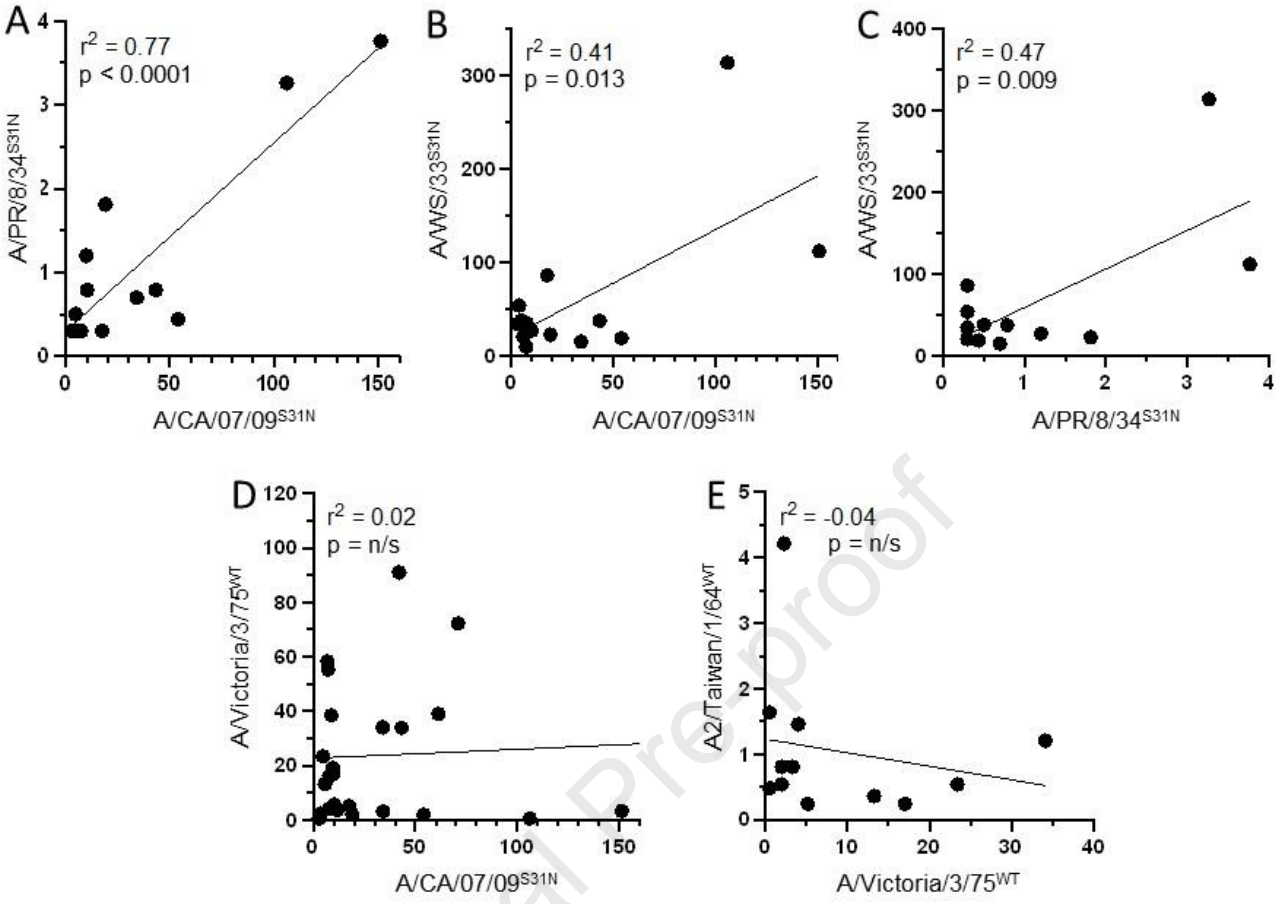

F r^2 values	A/PR/8/34^{S31N}	A/WS/33^{S31N}	A/Victoria/3/75^{WT}	A2/Taiwan/1/64^{WT}
A/CA/07/09^{S31N}	0.77	0.41	0.02	0.00
A/PR/8/34^{S31N}		0.47	0.06	0.00
A/WS/33^{S31N}			0.13	0.03
A/Victoria/3/75^{WT}				0.04

Figure 2. Comparisons of compound EC_{50}s (in µM) across viruses in **Table 1**. **A-E,** Representative comparisons of EC_{50}s of A/PR/8/34^{S31N} vs. A/CA/07/09^{S31N} (**A**), A/WS/33^{S31N} vs. A/CA/07/09^{S31N} (**B**), A/WS/33^{S31N} vs. A/PR/8/34^{S31N} (**C**), A/Victoria/3/75^{WT} vs. A/CA/07/09^{S31N} (**D**), and A2/Taiwan/1/64^{WT} vs. A/Victoria/3/75^{WT} (**E**). **F,** Summary of all correlations. For each comparison, at least 12 compounds were assessed including *Rmt*(**2**). Blue shading denotes r^2 values with a linear regression p-value < 0.05. n/s, non-significant.

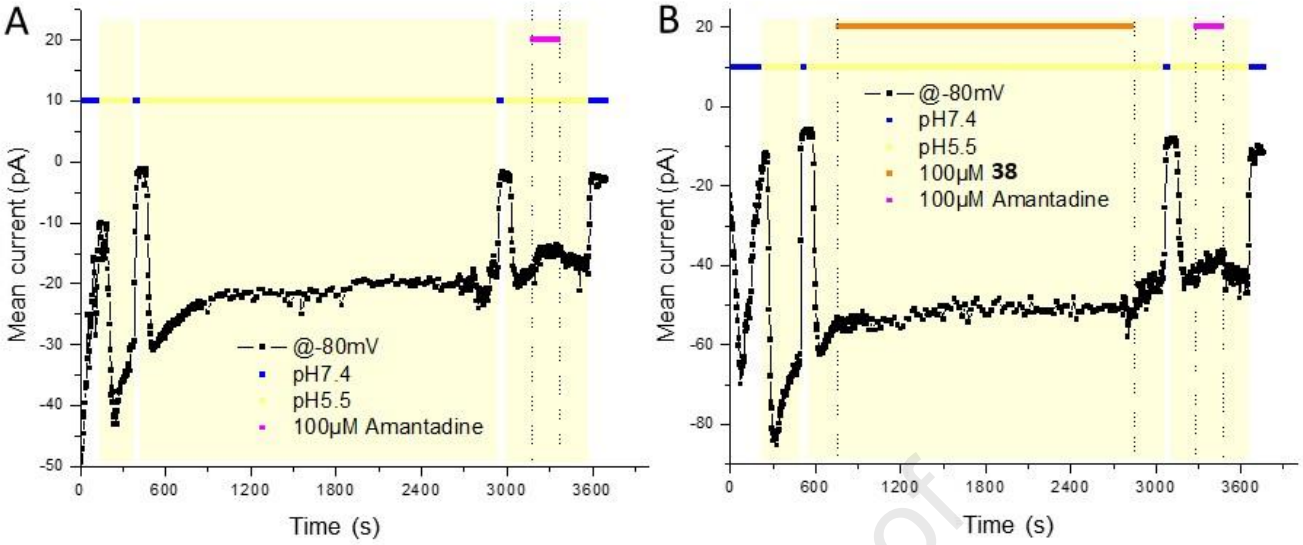

Figure 3. Representative diary plots of pH-dependent currents detected at -80 mV from single tsA-201 cells transiently expressing GFP and $M2^{S31N}$ (A/CA/07/09^{S31N}). Dots denote currents recorded at -80 mV every 4 seconds. Colors denote extracellular pH and addition of compounds. Effects of *Amt*(**1**) (**A**) and compound **38** (**B**) are shown.

638

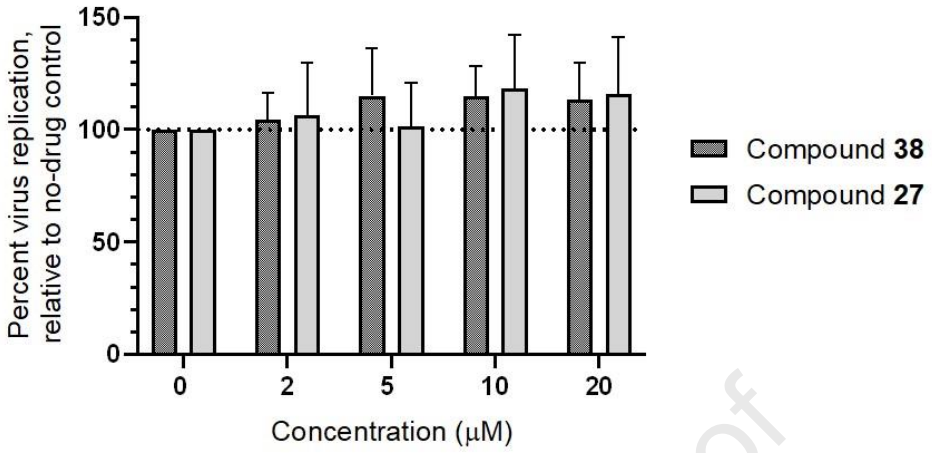

639 **Figure 4.** *Amt*(**1**) analogs do not inhibit BPV replication, in contrast to control antivirals that
640 selectively act through increasing endosomal pH. Results denote mean ± SD of four
641 independent experiments.

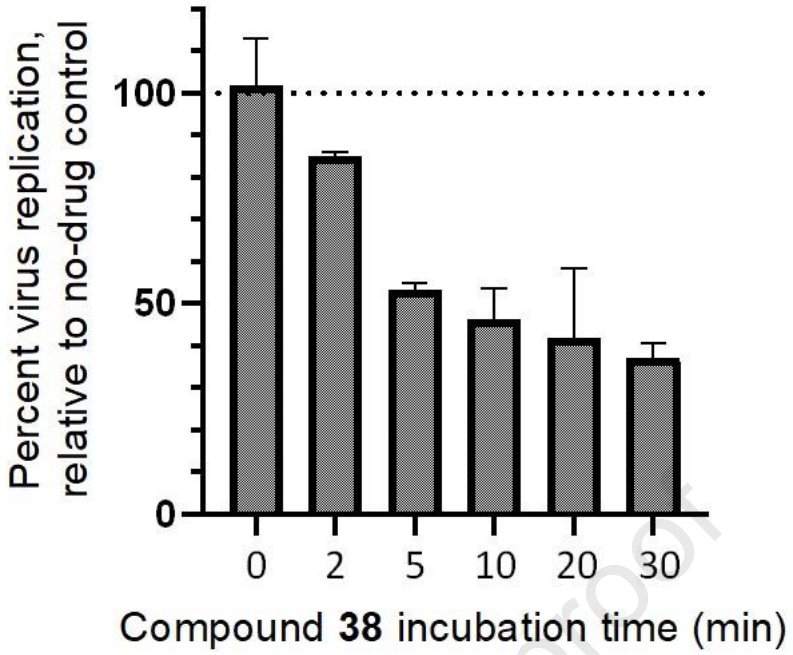

642

643 **Figure 5.** Compound **38** inhibits infectivity of influenza virus with $M2^{S31N}$. A/CA/07/09^{S31N} virus
644 was incubated with 50 μM of compound **38** at defined time intervals before infection of MDCK
645 cells. Results denote mean ± SD from two independent experiments.

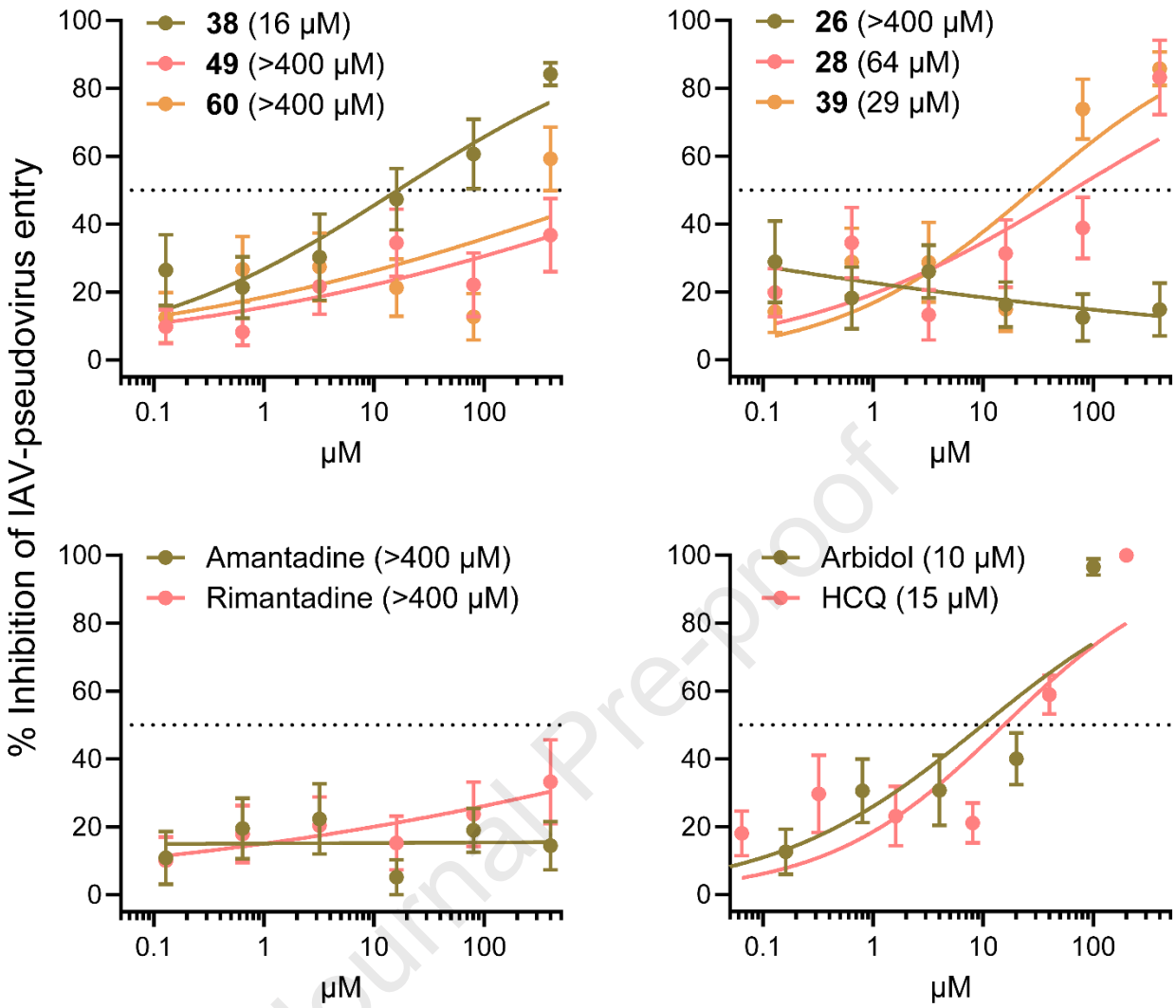

646

647 **Figure 6.** Inhibition of H1N1 pseudovirus entry by a selection of *Amt*(**1**) analogs. Pseudovirus
648 bearing the HA and NA proteins from A/H1N1/Virginia/ATCC3/2009 virus was transduced into
649 MDCK cells in the presence of the compounds. After three days incubation, the luciferase
650 readout was conducted. In each panel, the EC_{50} values are shown in brackets. Each data point
651 shows the mean ± SEM of nine values (three independent experiments, each performed in
652 triplicate). HCQ: hydroxychloroquine.

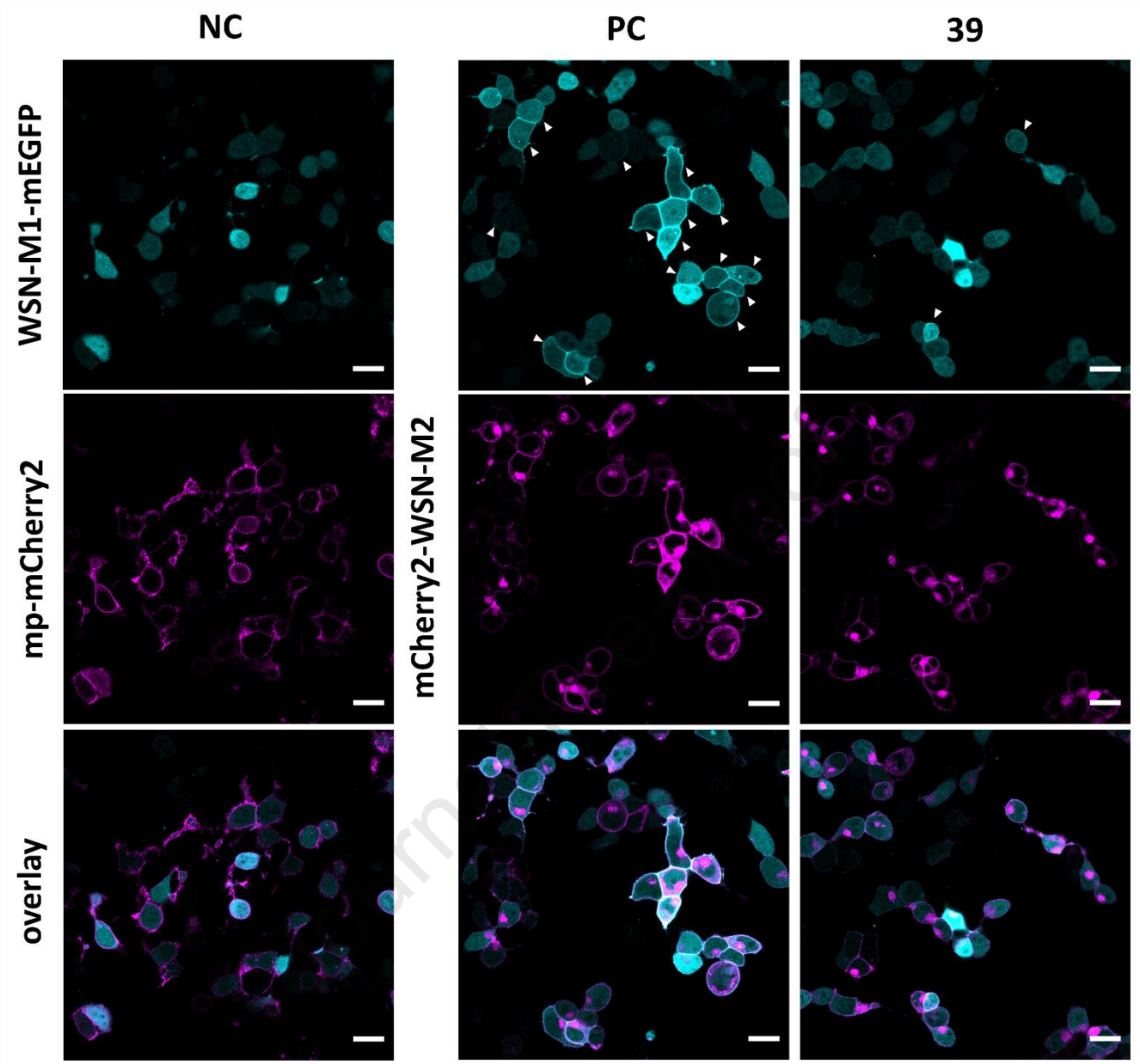

653 **Figure 7.** Membrane recruitment of influenza A virus matrix protein 1 (M1) in matrix protein 2
654 (M2) co-transfected cells is altered by *Amt*(**1**) analogs. Representative confocal fluorescence
655 images of HEK-293T cells co-expressing WSN-M1-mEGFP (cyan) (from A/H1N1/WSN/1933)
656 and either plasma membrane-associated mCherry2 (mp-mCherry2, as negative control (NC)),
657 or HA_{sp}-mCherry2-WSN-M2 (magenta). The latter samples were treated either with H_2O (as
658 positive control (PC)), or 30 µM of compound **39**. Imaging acquisition took place after 24 hours.

659 The lower panels show the two channels merged into a single image. Images for compounds
660 **38**, **49**, **60**, **26** and **28** at 30 µM are shown in the supporting material (**Figure S1**). White arrows
661 indicate cells with M1 plasma membrane (PM) localization. Intensity ranges were calibrated 2
662 to 100 for WSN-M1-mEGFP and HA_{sp}-mCherry2-WSN-M2. Scale bars represent 20 µm.

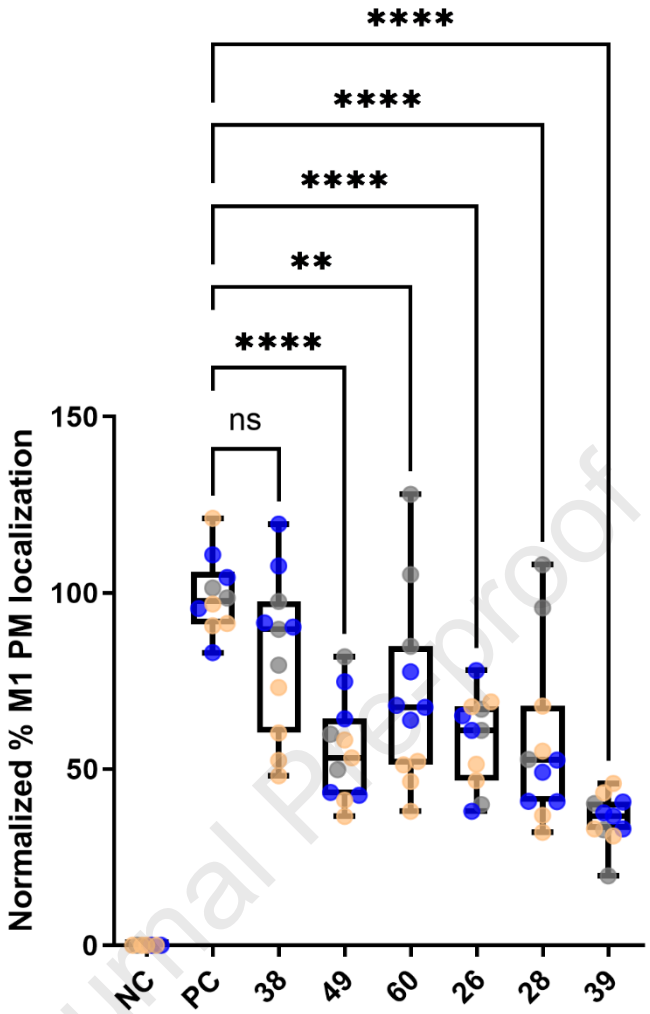

Figure 8. Quantification of IAV M1 recruitment to the PM by M2 in the presence of *Amt*(1) analogs. The plot shows the normalized percentage of cells displaying PM localization of M1 for the indicated treatment. A concentration of 30 µM was used for all compounds and imaged after 24 hours. The percentage of cells displaying M1 signal at the PM was manually identified using Fiji ImageJ software and the ratio of these cells to the total number of cells was calculated. This value was then normalized to the median value of the positive control (PC). Data from three separate experiments were pooled, plotted, and analyzed using a one-way ANOVA Dunnett's multiple comparison test (** $p < 0.01$, **** $p <$

671 0.0001). Each data point represents the percentage value measured for one image and the
672 colors of each point represent an individual experiment (experiment 1 (grey), 2 (blue) and 3
673 (orange)). Descriptive statistics are summarized in the supporting material (**Table S1**).

Declaration of interests

☒ The authors declare that they have no known competing financial interests or personal relationships that could have appeared to influence the work reported in this paper.

☐ The author is an Editorial Board Member/Editor-in-Chief/Associate Editor/Guest Editor for *[Journal name]* and was not involved in the editorial review or the decision to publish this article.

☐ The authors declare the following financial interests/personal relationships which may be considered as potential competing interests: